

The Ability of Significant Tidal Stress to Initiate Plate Tectonics

J.J. Zanazzi^{a,b,c}, Amaury H.M.J. Triaud^d

^a*Canadian Institute for Theoretical Astrophysics, University of Toronto, 60 St George Street, ON M5S 3H8, Canada*

^b*Cornell Center for Astrophysics, Planetary Science, Department of Astronomy, Cornell University, Ithaca, NY 14853, USA*

^c*Carl Sagan Institute, Cornell University, Ithaca, NY 14853, USA*

^d*School of Physics & Astronomy, University of Birmingham, Edgbaston, Birmingham B15 2TT, United Kingdom*

Abstract

Plate tectonics is a geophysical process currently unique to Earth, has an important role in regulating the Earth's climate, and may be better understood by identifying rocky planets outside our solar system with tectonic activity. The key criterion for whether or not plate tectonics may occur on a terrestrial planet is if the stress on a planet's lithosphere from mantle convection may overcome the lithosphere's yield stress. Although many rocky exoplanets closely orbiting their host stars have been detected, all studies to date of plate tectonics on exoplanets have neglected tidal stresses in the planet's lithosphere. Modeling a rocky exoplanet as a constant density, homogeneous, incompressible sphere, we show the tidal stress from the host star acting on close-in planets may become comparable to the stress on the lithosphere from mantle convection. Tidal stress of this magnitude may aid mantle convection stress in subduction of plates, or drive the subduction of plates without the need for mantle convective stresses. We also show that tidal stresses from planet-planet interactions are unlikely to be significant for plate tectonics, but may be strong enough to trigger Earthquakes. Our work may imply planets orbiting close to their host stars are more likely to experience plate tectonics, with implications for exoplanetary geophysics and habitability. We produce a list of detected rocky exoplanets under the most intense stresses. Atmospheric and topographic observations may confirm our predictions in the near future. Investigations of planets with significant tidal stress can not only lead to observable parameters linked to the presence of active plate tectonics, but may also be used as a tool to test theories on the main driving force behind tectonic activity.

Keywords: Extra-Solar Planets, Geophysics, Tectonics, Terrestrial planets, Tides, solid body.

Email addresses: jzanazzi@cita.utoronto.ca (J.J. Zanazzi), a.triaud@bham.ac.uk (Amaury H.M.J. Triaud)

1. Introduction

Plate tectonics plays a critical role in regulating the Earth’s climate. Mineral weathering continually reduces the amount of carbon dioxide in the Earth’s atmosphere, storing carbon dioxide in the crust (Southam et al., 2015). When plate tectonics pushes the Earth’s crust into the mantle (subduction), this carbon dioxide is re-released into the atmosphere through volcanism. For this reason, tectonics may play a critical role in maintaining life here on Earth (Kasting et al. 1993; Kopparapu et al. 2014, although see Tosi et al. 2017).

Because plate tectonics plays such a crucial role on the Earth’s climate, whether or not terrestrial planets can sustain plate tectonics is relevant for studies of exoplanetary climates and habitability. The criterion for determining if a terrestrial planet may undergo plate tectonics is if the stresses on a planet’s lithosphere from mantle convection may overcome the yield stress of the lithosphere to initiate subduction (Korenaga, 2013). If this condition is not met, the lithosphere behaves as a single, rigid plate on top of the convecting mantle below (the stagnant lid regime). In our own solar system, the Earth has active plate tectonics, while Mercury, Venus, and Mars have stagnant lids (Gregg, 2015).

The discovery of Super-Earths (planets with masses $1 M_{\oplus} < M \lesssim 10 M_{\oplus}$; Batalha et al. 2011) led many to consider the possibility of plate tectonics on exoplanets. Some early studies argued plate tectonics was impossible, since the gravity on super-Earths would make the lithosphere’s yield stress quite large (O’Neill and Lenardic, 2007). Other early studies argued plate tectonics was inevitable, using simulations and analytic arguments to scale different properties of the rocky super-Earth with mass, and showing mantle convective stresses can easily overcome the lithosphere’s yield stress. Later studies argued the planet’s mass played a near-negligible role compared to the influence of water reducing the planet’s lithospheric yield stress (Korenaga, 2010). Numerous theoretical and numerical works have followed, some of which see mobile plate-like behavior in their models, while others do not (Kite et al., 2009; Valencia and O’Connell, 2009; van Summeren et al., 2011; Foley et al., 2012; O’Rourke and Korenaga, 2012; Stamenković et al., 2012; Weller and Lenardic, 2012; Noack and Breuer, 2014).

Many transit surveys are targeting M-dwarf stars, because temperate terrestrial exoplanets are easier to detect around them due to their close ($\lesssim 0.1$ au) orbital semi-major axis (Nutzman and Charbonneau, 2008; Shields et al., 2016). M dwarfs are particularly interesting since they improve their planets’ odds to transit for a given incident flux (transits will happen dozens of times per year), while producing signals that can be up to two orders of magnitude stronger (including atmospheric signatures) compared to comparable planets orbiting single Sun-like stars (Rodler and López-Morales, 2014; Barstow and Irwin, 2016; Morley et al., 2017; He, Triaud and Gillon, 2017).

From exoplanetary statistics, we can infer $\sim 50\%$ of all stars with effective temperatures cooler than 4000° K harbor terrestrial planets (Dressing and Char-

bonneau, 2013; Bonfils et al., 2013; Dressing and Charbonneau, 2015; Morton and Swift, 2014; He, Triaud and Gillon, 2017), with $\sim 20\%$ of these planets expected to be in the habitable-zone (Morton and Swift, 2014; Dressing and Charbonneau, 2015), with some estimates pointing to higher fractions (Bonfils et al., 2013; He, Triaud and Gillon, 2017). The temperate TRAPPIST-1 planetary system (Gillon et al., 2016, 2017), as well as Proxima Centauri b (Anglada-Escudé et al., 2016) and Ross 128 b (Bonfils et al., 2017), have already been discovered orbiting M-dwarf stars. Due to the influence of plate tectonics on a planet’s climate, whether rocky planets (habitable or not) around an M-dwarf stars may support active plate tectonics is of great interest.

Super-Earths and sub-Neptune mass planets are frequent: planets more massive than Earth are encountered revolving around roughly half of Sun-like stars (Mayor et al., 2011; Howard et al., 2012), and 70-80% of M dwarfs (Bonfils et al., 2013), orbiting their host stars closer than Mercury orbits our Sun. Recent results examining the *Kepler* data point out which planets of this population are likely to be rocky ($R < 1.5R_{\oplus}$, $m < 4.5M_{\oplus}$; Rogers 2015; Fulton et al. 2017; Owen and Wu 2017; Ginzburg et al. 2017), raising the possibility of plate tectonics on these planets. A sub-population, called hot super-Earths, are planets with periods of order a few days (e.g. Fischer et al. 2008; Dawson and Fabrycky 2010). Because of their proximity to their host stars, these planets are likely tidally locked, with a large temperature contrast between the day and night sides of $\sim 1000^{\circ}\text{K}$ (Léger et al., 2011; Castan and Menou, 2011; Demory et al., 2016). Since a planet’s viscosity is temperature dependent, the day and night sides of these planets may have different tectonic activity, with a fully convective dayside without a rigid lithosphere, while the nightside may be able to sustain plate tectonics (van Summeren et al., 2011).

Many super Earths exist in multi-planetary system, called Systems of Tightly-packed Inner Planets, such as Kepler-11 (Lissauer et al., 2011), Kepler-33 (Lissauer et al., 2012), Kepler-32 (Swift et al., 2013), Kepler-80 (MacDonald et al., 2016), and Kepler-444 (Campante et al., 2015). STIPs are characterized by multiple planets orbiting their host stars at distances smaller than Mercury’s semi-major axis, and often have close encounters with other planets at distances $< 0.03\text{ au}$ that can excite their orbital eccentricities, or move them out of tidal synchronization (Vinson and Hansen, 2017; Delisle et al., 2017).

Although some studies considered plate tectonics on close-in, tidally locked exoplanets (van Summeren et al., 2011), the ability of tides to drive mantle convection (Barnes et al., 2009; Papaloizou et al., 2017), as well as the influence of tides on aquatic life (Sleep, 2012; Balbus, 2014; Lingam and Loeb, 2017), all works to date have neglected the influence of tidal stress in a terrestrial planet’s lithosphere. As we will show, this may not be a good approximation. The tidal influence of the host star on slightly eccentric planets with periods of order a day, as well as planets rotating non-synchronously, will generate stresses on exoplanetary lithospheres comparable to stresses from mantle convection. Tidal stresses of this magnitude may effectively weaken the planet’s lithosphere aiding mantle convective stresses in subducting plates, or drive the subduction of plates without the need for mantle convective stresses, and help initiate plate

tectonics on exoplanets. We will also consider the tidal stress acting on a planet from a close passage by another planet, which may also aid tectonic activity in terrestrial exoplanets. Section 2 sets up the model which we will use to calculate tidal stresses acting on a rocky exoplanet. Section 3 explicitly calculates the forces exerted on a lithospheric plate by mantle convection and tidal stress, and discusses under what conditions these forces may overcome frictional forces and subduct plates. Section 4 applies this model to non-synchronously rotating exoplanets, slightly eccentric ultra-short period planets, and systems of tightly packed inner planets. Section 5 discusses theoretical uncertainties in our analysis, as well as implications of our work. In Section 6 we briefly describe various observing methods that may confirm our predictions, as well a pathway to investigate plate tectonics in regimes where tidal stresses are less relevant. Section 7 summarizes our results.

2. Model of Tidally Stressed Elastic Exoplanet

We model the exoplanet as a constant density, incompressible sphere of mass m , radius R , and density ρ . The Maxwell stress tensor, encapsulating the internal stresses of the planet, is given by (Landau and Lifshitz, 1959b):

$$\mathbf{T} = p\mathbf{I} + 2\mu\mathbf{u}. \quad (1)$$

Here p is the pressure, \mathbf{I} the identity matrix, μ is the planet's shear modulus¹, while \mathbf{u} is the (incompressible) planet's strain tensor:

$$\mathbf{u} = \frac{1}{2}[(\nabla \cdot \boldsymbol{\xi}) + (\nabla \cdot \boldsymbol{\xi})^T], \quad (2)$$

where $\boldsymbol{\xi}$ is the displacement of the body from equilibrium. We assume the planet is homogeneous ($\mu = \text{constant}$).

The planet is tidally perturbed by a body of mass m' and distance $d \gg R$, with potential

$$\phi' \simeq \left(\frac{r}{R}\right)^2 \sum_{m=-2}^2 \Phi'_{2m} Y_{2m}(\theta, \varphi). \quad (3)$$

Here,

$$\Phi'_{2m} = \frac{4\pi G m' R^2}{5d^3} Y_{2m}^* \left(\frac{\pi}{2}, 0\right), \quad (4)$$

Y_{lm} are spherical harmonics (with θ and φ polar and azimuthal angles, respectively), and d is the distance of the planet from the perturber.

¹The shear modulus has units of pressure, and is a material property related to how the planet responds to shear stress. The higher the planet's shear modulus, the lower the deformation when shear stress is applied to a planet

We take hydrostatic equilibrium to be a state without shear stress. The equations of hydrostatic equilibrium are

$$-\frac{dp}{dr} - \rho \frac{d\phi}{dr} = 0 \quad (5)$$

$$\frac{1}{r^2} \frac{d}{dr} \left(r^2 \frac{d\phi}{dr} \right) = 4\pi G \rho, \quad (6)$$

where ϕ is the planet's gravitational potential. The boundary conditions are $d\phi/dr|_{r=0} = 0$ and $p(R) = 0$. One may show the solutions for ϕ and p are

$$\phi(r) = -\pi G \rho \left(2R^2 - \frac{2}{3} r^2 \right), \quad (7)$$

$$p(r) = \frac{2\pi}{3} G \rho^2 (R^2 - r^2). \quad (8)$$

The planet's state of hydrostatic equilibrium is disturbed by the tidal influence of the perturber, requiring internal stresses to resist its influence. For an incompressible, constant density, homogeneous sphere, the perturbed equations of elastostatic equilibrium are ([Landau and Lifshitz, 1959b](#))

$$-\nabla \delta p + \mu \nabla^2 \boldsymbol{\xi} - \rho \nabla (\delta \phi + \phi') = 0, \quad (9)$$

$$\nabla \cdot \boldsymbol{\xi} = 0, \quad (10)$$

$$\nabla^2 \delta \phi = 0, \quad (11)$$

where δp and $\delta \phi$ are the Eulerian perturbations to the planet's pressure and gravitational potential, respectively. Equations (9)-(11) are solved with the boundary conditions $\boldsymbol{\xi}(0) = 0$, the perturbed gravitational potential $\delta \phi$ is continuous at $r = R$, the first radial derivative of the Lagrangian perturbation to the gravitational potential is continuous at $r = R$, or

$$\left(\frac{\partial \delta \phi}{\partial r} + 4\pi G \rho \hat{\mathbf{r}} \cdot \boldsymbol{\xi} \right)_{r=R^-} = \left(\frac{\partial \delta \phi}{\partial r} \right)_{r=R^+}, \quad (12)$$

and the radial traction vanishes at the surface of the planet, or

$$\hat{\mathbf{r}} \cdot \Delta \mathbf{T}(R) = \left\{ -\delta p \hat{\mathbf{r}} + \mu \hat{\mathbf{r}} \cdot [(\nabla \boldsymbol{\xi}) + (\nabla \boldsymbol{\xi})^T] - (\boldsymbol{\xi} \cdot \nabla p) \hat{\mathbf{r}} \right\}_{r=R} = 0. \quad (13)$$

The solution for $\boldsymbol{\xi}$ may be decomposed in the form (see [Zanazzi and Lai 2017](#))

$$\boldsymbol{\xi} = \sum_{m=-2}^2 [\xi_{r;2m} Y_{2m} \hat{\mathbf{r}} + \xi_{\perp;2m} r \nabla Y_{2m}], \quad (14)$$

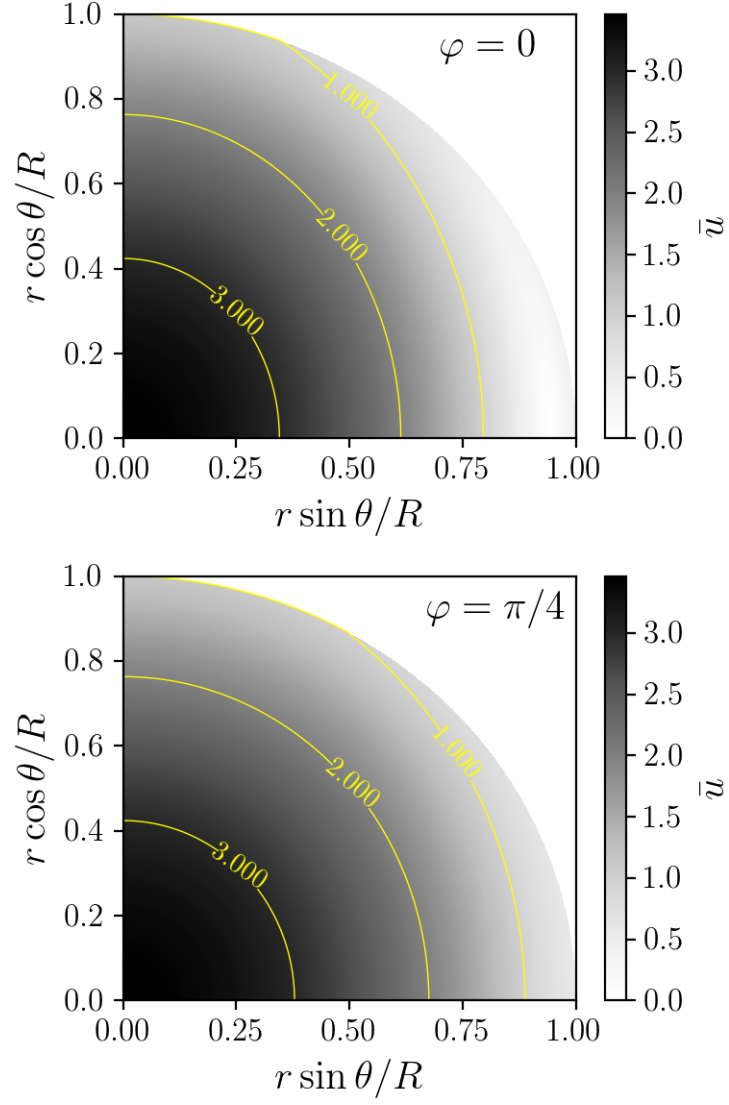


Figure 1: Color map of the re-scaled strain magnitude \bar{u} [Eq. (28)] inside the planet, with yellow contours tracing the specific values of \bar{u} indicated.

where

$$\xi_{r;2m} = \xi_{1m} \left(\frac{r}{R} \right)^3 + 2\xi_{3m} \left(\frac{r}{R} \right) \quad (15)$$

$$\xi_{\perp;2m} = \xi_{2m} \left(\frac{r}{R} \right)^3 + \xi_{3m} \left(\frac{r}{R} \right), \quad (16)$$

with ξ_{im} being constants determined by the planet's boundary conditions. In addition, we may decompose

$$\delta\phi = \sum_{m=-2}^2 \Phi_{2m} \left(\frac{r}{R} \right)^2 Y_{2m}(\theta, \varphi), \quad (17)$$

$$\delta p = \sum_{m=-2}^2 P_{2m} \left(\frac{r}{R} \right)^2 Y_{2m}(\theta, \varphi), \quad (18)$$

with Φ_{2m} and P_{2m} being undetermined constants. Applying the boundary conditions [Eq. (12)-(13)], the solution for the constants are

$$P_{2m} = \frac{2\bar{\mu}/19 - 5/2}{\bar{\mu} + 1} \rho \Phi'_{2m}, \quad (19)$$

$$\xi_{1m} = \frac{3/2}{\bar{\mu} + 1} \frac{\Phi'_{2m}}{g} \quad (20)$$

$$\xi_{2m} = \frac{5/4}{\bar{\mu} + 1} \frac{\Phi'_{2m}}{g} \quad (21)$$

$$\xi_{3m} = -\frac{2}{\bar{\mu} + 1} \frac{\Phi'_{2m}}{g} \quad (22)$$

$$\Phi_{2m} = \frac{3/2}{\bar{\mu} + 1} \Phi'_{2m}, \quad (23)$$

where $g = Gm/R^2$, and the re-scaled rigidity $\bar{\mu}$ is given by

$$\bar{\mu} \equiv \frac{19\mu}{2\rho g R} \quad (24)$$

$$= 2.038 \left(\frac{\mu}{10^{12} \text{ dynes/cm}^2} \right) \left(\frac{R}{R_{\oplus}} \right)^4 \left(\frac{m}{M_{\oplus}} \right)^{-2}. \quad (25)$$

We define the dimensionless tidal bulge

$$h \equiv \frac{GMR}{gd^3(1 + \bar{\mu})}, \quad (26)$$

and strain amplitude u via

$$u^2 \equiv \frac{1}{2} \text{Tr}(\mathbf{u} \cdot \mathbf{u}), \quad (27)$$

where $\text{Tr}(\mathbf{U})$ denotes the trace of the tensor \mathbf{U} . In the Appendix, we explicitly

calculate u [Eq. (27)] assuming ξ has the form (14). The magnitude of the strain amplitude $u(r, \theta, \varphi)$ represents how deformed the planet is under the influence of tidal stress. Since $u \propto h$, we also define the re-scaled strain amplitude

$$\bar{u} \equiv u/h. \quad (28)$$

In Figure 1, we plot the re-scaled strain amplitude \bar{u} for the elastic planet, perturbed by the tidal potential from the planet's host star. On the surface ($r = R$), the re-scaled strain amplitude reaches a maximum of

$$\max_{r=R, \theta, \varphi} [\bar{u}(r, \theta, \varphi)] = 1.15, \quad (29)$$

while deep in the core ($r \sim 0$), the re-scaled strain amplitude reaches a maximum of

$$\max_{r, \theta, \varphi} [\bar{u}(r, \theta, \varphi)] = 3.46. \quad (30)$$

From Fig. 1, we see the re-scaled strain \bar{u} is of order unity almost everywhere in the planet's interior, except at $(r, \theta) \approx (R, 0)$. Since $u = h\bar{u}$, tidal stress causes the planet to undergo strains u of order h almost everywhere in the planet.

When the planet's strain amplitude u exceeds a critical value u_{crit} somewhere in the planet's interior, the planet can no longer maintain elasto-static equilibrium, and begins to permanently deform under the influence of the external stress acting on the planet (the von Mises yield criterion, see [Turcotte and Schubert 2002](#)). The main driver of deformation on the Earth's lithosphere is mantle convection, which can exert shear stress exceeding $\tau_{\text{conv}} \gtrsim 10^7$ dynes/cm² [see Eq. (31)], but the value of τ_{conv} and exactly how it deforms the lithosphere is highly uncertain (see Sec. 3 for a discussion). We take the liberal assumption that interesting tectonic activity will occur when $h \gtrsim u_{\text{crit}} \sim \tau_{\text{conv}}/\mu \gtrsim 10^{-5}$ (assuming $\mu \sim 10^{12}$ dynes/cm²). In the next section, we explicitly calculate the forces these tidal stresses will exert on an exoplanet's lithospheric plates, and speculate on the conditions required for these forces to aid and/or hinder tectonic activity.

3. Conditions for Initiation of Plate Tectonics

In order for a planet to undergo plate tectonics, a lateral force must push one lithospheric plate under another at a fault line (subduction). This lateral force must overcome the frictional force acting between the two plates. On Earth, the main lateral force is driven by stresses acting on the lithosphere from mantle convection. This section shows under certain conditions, tidal stress may also drive subduction on extra-solar planets.

Before we discuss how tidal stress can initiate subduction, we review how stresses from mantle convection drive subduction on Earth (and potentially other planets as well). Consider the Earth with an upper mantle of depth D , viscosity η , and a characteristic convective velocity v_{conv} under a lithospheric plate of length and width L , and thickness δ (see Fig. 2 for setup). Plates

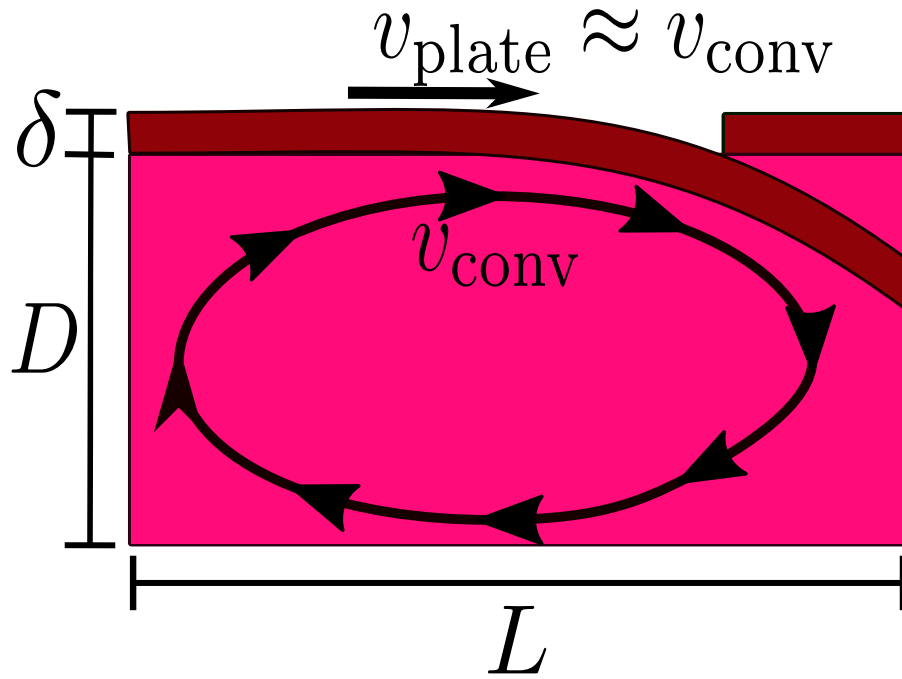


Figure 2: The setup for subduction of a planet's lithosphere from mantle convection. Here, v_{conv} is the characteristic convective velocity in the planet's mantle, D is the depth of the mantle's convective region, L is the plate length, δ is the plate thickness, and v_{plate} is the plate velocity.

and convective cells satisfy $\delta \ll L, D \ll R$ on Earth, so we may define a local cartesian frame with $\hat{\mathbf{z}} = \hat{\mathbf{r}}$, $\hat{\mathbf{x}} = \hat{\boldsymbol{\theta}}$, and $\hat{\mathbf{y}} = \hat{\boldsymbol{\varphi}}$, and neglect how the planet's curvature affects stress and forces between plates. We take $z = 0$ to lie on the planet's surface ($r = R$), and $x = y = 0$ to lie in the center of the square plate ($-L/2 \leq x, y \leq L/2$). Because the shear-stress from a fluid's viscosity η is of order $\tau_{\text{visc}} \sim \eta |\nabla \mathbf{v}|$ (\mathbf{v} is the fluid velocity), the shear stress on the Earth's lithosphere from mantle convection is of order

$$\begin{aligned} \tau_{\text{conv}} &\sim \eta v_{\text{conv}} / D \\ &= 2.3 \times 10^6 \left(\frac{\eta}{10^{21} \text{ poises}} \right) \left(\frac{v_{\text{conv}}}{5 \text{ cm/yr}} \right) \left(\frac{D}{700 \text{ km}} \right)^{-1} \text{ dynes/cm}^2. \end{aligned} \quad (31)$$

The lateral force on the lithosphere from mantle convection is then of order

$$\begin{aligned} F_{\text{conv}} &= \int_{-L/2}^{L/2} \int_{-L/2}^{L/2} \tau_{\text{conv}} dx dy \sim \frac{\eta v_{\text{conv}} L^2}{D} \\ &= 4.4 \times 10^{22} \left(\frac{\eta}{10^{21} \text{ poises}} \right) \left(\frac{v_{\text{conv}}}{5 \text{ cm/yr}} \right) \\ &\quad \times \left(\frac{L}{1400 \text{ km}} \right)^2 \left(\frac{D}{700 \text{ km}} \right)^{-1} \text{ dynes}. \end{aligned} \quad (32)$$

The main force resisting mantle convection forces are frictional forces between two sliding plates. The shear stress from friction acting on one plate sliding against another is (Byerlee, 1978; Moresi and Solomatov, 1998)

$$\tau_{\text{fric}} = \tau_0 + \lambda \rho g z, \quad (33)$$

where τ_0 is a cohesion parameter, and λ is the (dimensionless) friction coefficient. Since we expect $\tau_0 \ll \lambda \rho g \delta$ (Byerlee, 1978), we neglect τ_0 in τ_{fric} from now on. Silicate rocks typically have $\lambda \sim 0.6 - 0.8$ (Byerlee, 1978), but the (effective) friction coefficient may be lowered to $\lambda \sim 0.03$ on Earth's surface due to hydrostatic pore pressure (Korenaga, 2007). The frictional shear-stress exerts a lateral force between two plates of

$$\begin{aligned} F_{\text{fric}} &= \int_{-L/2}^{L/2} \int_{-\delta}^0 \tau_{\text{fric}} dz dy = \frac{\lambda}{2} \rho g \delta^2 L \\ &= 1.2 \times 10^{24} \left(\frac{\lambda}{0.03} \right) \left(\frac{\rho}{6 \text{ g/cm}^3} \right) \\ &\quad \times \left(\frac{g}{981 \text{ cm/s}^2} \right) \left(\frac{\delta}{100 \text{ km}} \right)^2 \left(\frac{L}{1400 \text{ km}} \right) \text{ dynes} \end{aligned} \quad (34)$$

The force in (34) acts in the $\hat{\mathbf{x}}$ direction: a force of equal magnitude acts in the $\hat{\mathbf{y}}$ direction as well. Comparing Equations (32) and (34), we see to initiate subduction on earth-like planets ($F_{\text{conv}} \gtrsim F_{\text{fric}}$), one requires λ to be weakened

below the values for dry silicate rocks ($\lambda \gtrsim 0.6$).

The convective stress (31) is many orders of magnitude lower than the yield stress of rocks which make up the Earth’s lithosphere ($\tau_{\text{yield}} \sim 10^9 - 10^{10}$ dynes/cm²), inferred through laboratory experiments (Kohlstedt et al., 1995). More detailed calculations using boundary-layer theory (e.g. Turcotte & Oxburgh 1967; Fowler 1993), as well as simulations of mantle convection (e.g. Trompert and Hansen 1998; van Heck and Tackley 2008; Foley and Becker 2009; Wong and Solomatov 2015) give estimates of τ_{conv} to be of order 10^8 dynes/cm². Even with τ_{conv} of this magnitude, in order to initiate subduction ($F_{\text{conv}} \gtrsim F_{\text{fric}}$), one requires a value of the friction coefficient λ to have a value far below that expected for lithospheric rocks ($\lambda \sim 0.6 - 0.8$, Byerlee 1978; Kohlstedt et al. 1995). How plate tectonics is initiated on Earth, given the stress on the Earth from mantle convection is so much lower than the lithosphere’s yield stress, is an outstanding problem in Geophysics (see Korenaga 2013 for a review).

There are two main ideas for how to initiate plate tectonics on Earth. One idea comes from laboratory experiments which show the presence of surface water can weaken the lithosphere’s yield stress. Experiments show minerals such as olivine which make up the Earth’s lithosphere are much weaker when wet (e.g. Karato et al. 1986; Mei and Kohlstedt 2000a,b). Another explanation is the simple pseudo-plastic rheologies used in simulations of plate tectonics are not realistic. Damage theory, which models the reduction and growth of grains in a planet’s lithosphere, may generate plate-like behavior with a realistic rheology (Bercovici and Ricard, 2003). Both effects would work to effectively reduce friction coefficient in Equation (33). Due to the uncertainty of how plate tectonics is initiated and sustained here on Earth, we leave λ to be a free parameter, and note weakening mechanisms must also operate on a planet’s lithosphere if the planet’s friction coefficient is low ($\lambda \sim 0.03$).

Tidal stress also exerts a lateral force on plates, and may potentially initiate subduction if sufficiently strong. Because the radial traction on the planet’s surface vanishes [see Eq. (13)], shear strains from tidal deformations are negligible in the planet’s lithosphere ($u_{r\theta} \sim u_{\varphi r} \lesssim h\delta/R$ when $R - \delta \leq r \leq R$). Therefore, the lateral force from tidal stress comes primarily from normal stresses exerting a lateral force F_t of order

$$\begin{aligned} F_t &\sim \mu h \delta L \\ &= 1.4 \times 10^{24} \left(\frac{\mu}{10^{12} \text{ dynes/cm}^2} \right) \left(\frac{h}{10^{-3}} \right) \\ &\quad \times \left(\frac{\delta}{100 \text{ km}} \right) \left(\frac{L}{1400 \text{ km}} \right) \text{ dynes.} \end{aligned} \quad (35)$$

Using the estimate for the tidal force acting on a lithospheric plate (35), we may

calculate two critical tidal bulges:

$$\begin{aligned}
h_{\text{conv}} &= \frac{F_{\text{conv}}}{\mu \delta L} \\
&\sim 3.2 \times 10^{-5} \left(\frac{\eta}{10^{21} \text{ poises}} \right) \left(\frac{v_{\text{conv}}}{5 \text{ cm/yr}} \right) \left(\frac{L}{1400 \text{ km}} \right) \\
&\quad \times \left(\frac{D}{700 \text{ km}} \right)^{-1} \left(\frac{\mu}{10^{12} \text{ dynes/cm}^2} \right)^{-1} \left(\frac{\delta}{100 \text{ km}} \right)^{-1}, \quad (36)
\end{aligned}$$

$$\begin{aligned}
h_{\text{fric}} &= \frac{F_{\text{fric}}}{\mu \delta L} \\
&\sim 8.8 \times 10^{-4} \left(\frac{\lambda}{0.03} \right) \left(\frac{\mu}{10^{12} \text{ dynes/cm}^2} \right)^{-1} \\
&\quad \times \left(\frac{\rho}{6 \text{ g/cm}^3} \right) \left(\frac{g}{981 \text{ cm/s}^2} \right) \left(\frac{\delta}{100 \text{ km}} \right). \quad (37)
\end{aligned}$$

When $h \gtrsim h_{\text{conv}}$, tidal stresses may significantly aid or hinder convective stresses in subducting plates. When $h \gtrsim h_{\text{fric}}$, tidal stresses may overcome frictional forces between two plates to initiate subduction without the aid of mantle convective stresses.

To understand how the tidal forces acting on plates vary across an earth-like planet's surface, we explicitly calculate $\mathbf{F}_t = F_{tx}\hat{\mathbf{x}} + F_{ty}\hat{\mathbf{y}}$ for our tidal model. Neglecting the contribution from $u_{r\theta}$ and $u_{\theta\varphi}$ in the lateral force from tidal stress, we have

$$\begin{aligned}
F_{tx} &= \int_{-L/2}^{L/2} \int_{-\delta}^0 \mu u_{\theta\theta}(x, y, z) dy dz + \int_{-L/2}^{L/2} \int_{-\delta}^0 \mu u_{\theta\varphi}(x, y, z) dx dz \\
&\simeq \mu \delta L [u_{\theta\theta}(0, 0, 0) + u_{\theta\varphi}(0, 0, 0)], \quad (38)
\end{aligned}$$

$$\begin{aligned}
F_{ty} &= \int_{-L/2}^{L/2} \int_{-\delta}^0 \mu u_{\theta\varphi}(x, y, z) dy dz + \int_{-L/2}^{L/2} \int_{-\delta}^0 \mu u_{\varphi\varphi}(x, y, z) dx dz \\
&\simeq \mu \delta L [u_{\theta\varphi}(0, 0, 0) + u_{\varphi\varphi}(0, 0, 0)], \quad (39)
\end{aligned}$$

where we have assumed the strain u_{ij} is approximately constant over the plate's volume. Figure 3 plots the magnitude of the tidal force components $|F_{tx}|$ and $|F_{ty}|$ of a plate centered at different locations across an earth-like planet's surface. We see when an earth-like planet undergoes significant tidal stress ($h \gtrsim 3 \times 10^{-4} - 10^{-3}$), tidal forces overcome the resisting frictional force (for low λ values) and may either aid mantle convective stresses in subducting plates, or initiate subduction outright over a substantial portion of the planet's surface.

Once a plate is subducted, buoyancy forces may pull the plate into the planet's mantle (Turcotte and Schubert, 2002). Consideration of what happens to a lithospheric plate after subduction is outside the scope of this work, since an estimate of buoyancy forces would require knowledge of a planet's thermal properties. However, we note that tidal stress will still be acting on a plate while

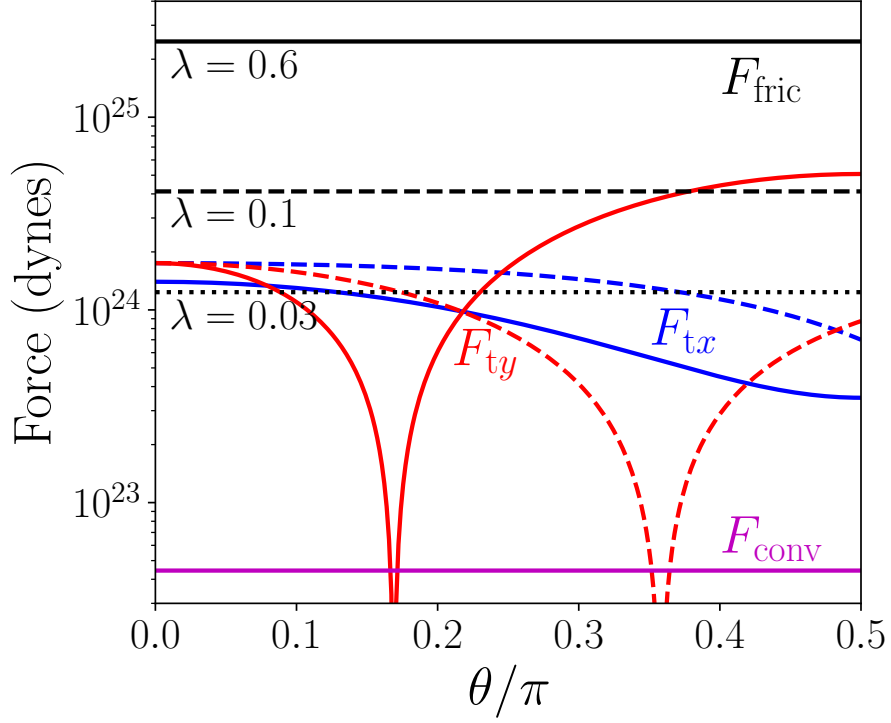


Figure 3: Absolute values of the tidal force components $|F_{tx}|$ [blue, Eq. (38)] and $|F_{ty}|$ [red, Eq. (39)] centered at the displayed polar angles θ , with azimuthal angle $\varphi = 0$ (solid lines) and $\varphi = \pi/4$ (dashed lines). Black lines denote the friction force F_{fric} [Eq. (34)] between two sliding plates, while the magenta line denotes the mantle convection force F_{conv} [Eq. (32)] acting on a lithospheric plate, with friction coefficients λ as indicated. Here, $\mu = 10^{12}$ dynes/cm², $h = 10^{-3}$, $\delta = 100$ km, $L = 1400$ km, $\rho = 6$ g/cm³, and $g = 981$ cm/s².

being pulled into a planet’s mantle (see Fig. 1), potentially helping or hindering the recycling of a lithosphere.

4. Exoplanets with High Tidal Stress

When considering how tidal stresses influence an elastic exoplanet undergoing mantle convection, three timescales need to be considered. The first is the time it takes an elastic shear wave to propagate over the entire planet (e.g. Quillen et al. 2016):

$$t_{\text{elast}} = \frac{R}{\sqrt{\mu/\rho}} = 1.81 \times 10^{-2} \left(\frac{R}{R_{\oplus}} \right) \left(\frac{\mu}{10^{12} \text{ dynes/cm}^2} \right)^{-1/2} \left(\frac{\rho}{6 \text{ g/cm}^3} \right)^{1/2} \text{ days}, \quad (40)$$

We assumed in Section 2 the planet lies in elasto-static equilibrium, which requires $h^{-1}|dh/dt| \ll t_{\text{elast}}^{-1}$. When $h^{-1}|dh/dt| \gtrsim t_{\text{elast}}^{-1}$, one needs to do a different calculation of the tidal stress on the planet using the impulse approximation (Quillen et al., 2016).

The second timescale is the time it takes a material to viscously relax to external stress (Maxwell time; Turcotte and Schubert 2002):

$$t_{\text{Max}} = \frac{\eta}{\mu} = 31.7 \left(\frac{\eta}{10^{21} \text{ poises}} \right) \left(\frac{\mu}{10^{12} \text{ dynes/cm}^2} \right)^{-1} \text{ years}, \quad (41)$$

where η is the material’s dynamic viscosity, which we have evaluated at the viscosity characteristic of the Earth’s upper mantle (Turcotte and Schubert, 2002). In order for the planet to not viscously relax to the tidal stress acting on the planet, we require $h^{-1}|dh/dt| \gg t_{\text{Max}}^{-1}$. Viscous relaxation will limit the ability of tidal stresses to cause plastic yielding in a planet’s lithosphere.

The last timescale is the turnover time of the largest convective eddies t_{conv} :

$$t_{\text{conv}} = \frac{D}{v_{\text{conv}}} = 1.4 \times 10^7 \left(\frac{5 \text{ cm/yr}}{v_{\text{conv}}} \right) \left(\frac{D}{700 \text{ km}} \right) \text{ years}, \quad (42)$$

which is comparable to the timescale over which a lithospheric plate moves ($t_{\text{plate}} \approx L/v_{\text{conv}} \sim t_{\text{conv}}$). Tidal stress/strains may influence the large-scale convective motions in the planet’s mantle when $h^{-1}|dh/dt| \lesssim t_{\text{conv}}^{-1}$. Since $t_{\text{conv}} \gg t_{\text{Max}}$ for the parameters of interest, any tidal stress which varies over the convective timescale will viscously relax before influencing convective motions in the planet.

This section directly applies our model to observed exoplanetary systems. We emphasize the degree to which we have idealized the interior structure of these planets: we assume a constant density incompressible planet, with a uniform shear modulus which takes a value characteristic of the Earth’s shear

modulus. More massive planets with rocky compositions will not be incompressible (e.g. Seager et al. 2007), and the shear modulus varies in magnitude within a body depending on the local pressure, temperature, and composition (e.g. Dziewonski et al. 1975; Yoder 1995; Turcotte and Schubert 2002). These approximations are reasonable given the level of knowledge on the interior structures and compositions of planets outside our solar system, but makes our calculation of tidal stress acting on a planet unreliable beyond an order of magnitude estimate. For this reason, we do not explicitly state our error bars with the estimated values of tidal stresses acting on exoplanets, even though the system’s parameters have well defined uncertainties.

In the following subsections, we will consider three examples which satisfy $t_{\text{Max}}^{-1} \ll h^{-1}|dh/dt| \ll t_{\text{elast}}^{-1}$: tides from the host stars of non-synchronously rotating planets in Habitable Zones of M-dwarf’s, tides from the host stars of slightly eccentric Ultra-Short Period (USP) planets, and tides from other planets in tightly packed planetary systems. The tidal stresses in these systems may aid or hinder tectonic activity when $h \gtrsim h_{\text{conv}} \sim 10^{-5}$ [see Eq. (36)].

4.1. Non-synchronously rotating planets

Because of their close proximities to their host stars, tides work to drive the rotation of planets toward synchronization with the planet’s orbital period. Planets may escape synchronous rotation through capture into a spin-orbit resonance (Goldreich and Peale, 1966; Makarov et al., 2012; Ribas et al., 2016), atmospheric tides (Correia et al., 2003; Leconte et al., 2015; Auclair-Desrotour et al., 2017), and resonant planet-planet interactions (Delisle et al., 2017; Vinson and Hansen, 2017). If this occurs, the (dimensionless) tidal bulge on the host star

$$h = \frac{1}{1 + \bar{\mu}} \left(\frac{M}{m} \right) \left(\frac{R}{a} \right)^3, \quad (43)$$

where M is the stellar mass and a is the planet’s orbital semi-major axis, will vary on a timescale

$$\frac{1}{h} \left| \frac{dh}{dt} \right| \sim \left| \frac{1}{P_{\text{orb}}} - \frac{1}{P_{\text{rot}}} \right|, \quad (44)$$

where P_{rot} is the rotation period of the planet’s spin, and P_{orb} is the planet’s orbital period. As long as $t_{\text{Max}} \gg |P_{\text{rot}}^{-1} - P_{\text{orb}}^{-1}|^{-1} \gg t_{\text{elast}}$, the tides on the planet from the host star will generate stress of order

$$h = \frac{1.6 \times 10^{-4}}{1 + \bar{\mu}} \left(\frac{M}{0.1 M_{\odot}} \right) \left(\frac{m}{1 M_{\oplus}} \right)^{-1} \left(\frac{R}{R_{\oplus}} \right)^3 \left(\frac{a}{0.025 \text{ au}} \right)^{-3}. \quad (45)$$

This tidal stress will exert a lateral force acting on a lithospheric plate, which will change in direction and magnitude as the close-in planet rotates non-synchronously

In Table 1, we list h for the temperate planets TRAPPIST-1 b, c, d, e, and f, as well as GJ 1132 b. We see $h \gtrsim 10^{-4} - 10^{-5}$ for all planets listed (assuming $\mu = 10^{12}$ dynes/cm²), implying tides may generate stresses of order the mantle

Planet	m (M_{\oplus})	R (R_{\oplus})	P_{orb} (days)	h ($\times 10^{-5}$)
TRAPPIST-1 b	0.86	1.06	1.51	46.49
TRAPPIST-1 c	1.38	1.03	2.42	21.11
TRAPPIST-1 d	0.41	0.76	4.05	4.47
TRAPPIST-1 e	0.64	0.90	6.10	2.46
TRAPPIST-1 f	0.67	1.02	9.21	1.08
GJ 1132 b	1.62	1.13	1.63	50.93

Table 1: TRAPPIST-1 (Gillon et al., 2017) and GJ 1132 b (Berta-Thompson et al., 2015) planetary properties and dimensionless tidal bulge h [Eq. (45)]. TRAPPIST-1 has a mass $M = 0.08 \pm 0.01 M_{\odot}$ (Gillon et al., 2017), while GJ 1132 has a mass $M = 0.181 \pm 0.002 M_{\odot}$ (Berta-Thompson et al., 2015). The planet’s semi-major axis is computed via $a = (2\pi/P_{\text{orb}})^{2/3}(GM)^{1/3}$, and we take $\mu = 10^{12}$ dynes/cm² for all bodies. We do not explicitly state uncertainties in the observational parameters and the calculated h values, because of the model uncertainties (see text for discussion).

convective stresses on these planets. We have looked through the [Extrasolar Planets Encyclopaedia](#) (Schneider et al., 2011), and found that 42 likely rocky ($R < 1.6 R_{\oplus}$, Rogers 2015; Fulton et al. 2017) exoplanets have $h > 10^{-5}$, whose tectonic activity could potentially be affected by tidal processes. We list these planets in Table B.3.

We will discuss the prospects for detecting evidence of plate tectonics in section 6, but we will point out here that the habitability of temperate planet can be affected by tectonics, and may play an important role in stabilizing a planet’s climate (e.g. Kasting et al. 1993; Kopparapu et al. 2014). The planets TRAPPIST-1 c, d, e, and f have equilibrium temperatures between 400° K and 150° K, considered temperate (Gillon et al., 2017).

4.2. Eccentric Ultra-Short Period Planets

Numerous super-Earth mass planets have been detected with orbital periods $P_{\text{orb}} < 1$ day, such as 55 Cnc e (Fischer et al., 2008; Dawson and Fabrycky, 2010; Nelson et al., 2014; Demory et al., 2016), CoRoT-7b (Léger et al., 2009; Bruntt et al., 2010; Haywood et al., 2014), Kepler 10b (Batalha et al., 2011; Esteves et al., 2015; Weiss et al., 2016), WASP-47e (Becker et al., 2015; Dai et al., 2015; Weiss et al., 2016; Sinukoff et al., 2017), K2 106b (Sinukoff et al., 2017; Guenther et al., 2017). Due to their close proximities to their host stars, USP planets will be tidally circularized and rotating synchronously with rotation periods equal to their orbital periods. This means the “equilibrium” tidal bulge

$$h_{\text{eq}} = \frac{1}{1 + \bar{\mu}} \left(\frac{M}{m} \right) \left(\frac{R}{a} \right)^3 \quad (46)$$

will satisfy $dh_{\text{eq}}/dt \simeq 0$, so h_{eq} will viscously relax and not stress the planet.

However, many of these USP planets have exterior planetary companions, which will pump the USP planet’s eccentricity, but theoretical value for USP planetary eccentricities is uncertain. One may delay the tidal damping of the USP planet’s eccentricity by orders of magnitude through secular planet-planet

interactions (Wu and Goldreich, 2002). Bolmont et al. (2013) argued planet-planet interactions may pump up the eccentricity of 55 Cnc e to $e \sim 10^{-3}$ - 10^{-2} . The combination of planet-planet interactions and exciting the USP planet's second gravitational moment (J_2) through tidal interactions with the host star, Rodríguez et al. (2016) argued the eccentricity of CoRoT-7b may be pumped up to $e \sim 0.1$. Although the magnitude of e is extremely uncertain, assuming a USP planet in a multi-planetary system has an eccentricity of order 10^{-2} is not unreasonable.

The small eccentricity e of the USP planet will cause h to vary by (assuming $e \ll 1$)

$$\Delta h \simeq \frac{6e}{1 + \bar{\mu}} \left(\frac{m}{M} \right) \left(\frac{R}{a} \right)^3 \quad (47)$$

over the planet's orbital period P_{orb} , so

$$\frac{1}{\Delta h} \left| \frac{d\Delta h}{dt} \right| \sim \frac{1}{P_{\text{orb}}}. \quad (48)$$

Since $t_{\text{Max}} \gg P_{\text{orb}} \gg t_{\text{elast}}$ for an USP planet, the variation Δh of the tidal bulge will cause stress in the planet. Evaluating Eq. (47) for parameters characteristic of USP planets, we see

$$\Delta h = \frac{3.8 \times 10^{-4}}{1 + \bar{\mu}} \left(\frac{e}{0.01} \right) \left(\frac{M}{1 M_{\odot}} \right) \left(\frac{m}{5 M_{\oplus}} \right)^{-1} \left(\frac{R}{1.6 R_{\oplus}} \right)^3 \left(\frac{a}{0.015 \text{ au}} \right)^{-3}. \quad (49)$$

Since $\Delta h \gtrsim 10^{-4}$ for a wide range of USP planet parameter space, we expect the tidal bulge variation due to the planet's small but non-zero eccentricity to cause stress comparable to the convective stresses on the planet's lithosphere. This tidal stress will exert a lateral force on an USP planet's lithospheric plate, and the lateral force will switch direction every half orbital period.

Table 2 lists the parameters for a number of ultra-short period (USP) planets, with the time-varying tidal bulge Δh [Eq. (47)] rescaled to the orbital eccentricity $e = 0.01$. Some of these planets have measured eccentricities, such as 55 Cnc e ($e = 0.028^{+0.022}_{-0.019}$; Nelson et al. 2014), CoRoT-7b ($e = 0.12 \pm 0.07$; Haywood et al. 2014), and WASP-47e ($e = 0.03 \pm 0.02$; Weiss et al. 2016). But because the detection of these planetary eccentricities is marginal, we leave the planet's eccentricity fixed to a conservative value of $e = 0.01$. We note that this exceeds the measured eccentricity of TRAPPIST-1 b ($e = 0.005 \pm 0.001$; Luger et al. 2017).

We also note that similar tidal stress should also be acting on Io, which is tidally synchronized with a small eccentricity, and displays tectonic activity

Planet	m (M_{\oplus})	R (R_{\oplus})	a (au)	M (M_{\odot})	$\Delta h \times (0.01/e)$
55 Cnc e	8.08	1.91	0.0154	0.95	2.5×10^{-4}
CoRoT-7b	4.45	1.58	0.0171	0.91	1.5×10^{-4}
Kepler-10b	3.76	1.47	0.0169	0.91	1.5×10^{-4}
WASP-47e	9.1	1.76	0.0167	1.00	1.6×10^{-4}
K2-106b	9.0	1.82	0.0131	0.92	3.6×10^{-4}

Table 2: Ultra-short period planetary properties in multiplanet systems, with a calculated time-varying dimensionless tidal bulge Δh [Eq. (47)]. We take $\mu = 10^{12}$ dynes/cm² for all bodies, and rescale Δh by $0.01/e$ due to uncertainties in the planetary orbital eccentricities (see text for discussion). Listed above are all Ultra-Short Period planets ($P_{\text{orb}} < 1$ day) with detected planetary companions. Planet and system parameters obtained from Demory et al. (2016) (55 Cnc e), Haywood et al. (2014) (CoRoT-7b), Esteves et al. (2015) (Kepler-10b), Sinukoff et al. (2017) (WASP-47e), and Sinukoff et al. (2017) (K2-106b).

(although *very* different from Earth’s, see Turtle et al. 2007 for a review):

$$\Delta h_{\text{Io}} = \frac{4.2 \times 10^{-5}}{1 + \bar{\mu}} \left(\frac{e}{0.0041} \right) \left(\frac{M}{M_{\text{Jup}}} \right) \left(\frac{0.015 M_{\oplus}}{m} \right) \times \left(\frac{R}{0.286 R_{\oplus}} \right)^3 \left(\frac{0.00282 \text{ au}}{a} \right)^3. \quad (50)$$

Since $\Delta h_{\text{Io}} \gtrsim 10^{-5}$, we speculate that the tidal stress from Jupiter may play a role in Io’s tectonic activity.

4.3. Tightly Packed Planetary Systems

Numerous planetary systems have been discovered in which the spacing between two planetary orbits is less than 0.1 au, such as Kepler-11 (Lissauer et al., 2011), Kepler-32 (Swift et al., 2013), Kepler-33 (Lissauer et al., 2012), Kepler-36 (Carter et al., 2012; Deck et al., 2012), Kepler-80 (MacDonald et al., 2016), Kepler-444 (Campante et al., 2015), and TRAPPIST-1 (Gillon et al., 2016, 2017). Assuming the planetary companion has a mass m_c and semi-major axis a_c , with both the planet and its companion in circular orbits, the magnitude of h at closest approach is

$$h = \frac{1}{1 + \bar{\mu}} \left(\frac{m_c}{m} \right) \left(\frac{R}{|a - a_c|} \right)^3. \quad (51)$$

Since $|a - a_c| \ll |a + a_c|$, h will vary by many orders of magnitude over an orbital period. For a planetary companion with orbital period P_c ,

$$\frac{1}{h} \left| \frac{dh}{dt} \right| \sim \left| \frac{1}{P_{\text{orb}}} - \frac{1}{P_c} \right|. \quad (52)$$

Calculating h for typical tightly packed planetary system parameters, we see

$$h = \frac{2.9 \times 10^{-6}}{1 + \bar{\mu}} \left(\frac{m_c}{m} \right) \left(\frac{R}{R_\oplus} \right)^3 \left(\frac{|a - a_c|}{0.003 \text{ au}} \right)^{-3}. \quad (53)$$

Even for very tightly packed planetary systems, $h \ll 10^{-5}$, so planet-planet tidal interactions are unlikely to affect the subduction of plates on a planet's lithosphere. However, planet-planet tidal stresses in systems of tightly packed planets are much greater than the stress on the Earth caused by the Moon:

$$h_{\oplus, \text{Moon}} = \frac{4.8 \times 10^{-8}}{1 + \bar{\mu}} \left(\frac{M}{M_{\text{Moon}}} \right) \left(\frac{m}{M_\oplus} \right)^{-1} \left(\frac{R}{R_\oplus} \right)^3 \left(\frac{a}{0.00271 \text{ au}} \right)^{-3}. \quad (54)$$

If tidal stresses help induce Earthquakes here on Earth, as suggested in [Ide et al. \(2016\)](#), planet-planet tides are likely to be a much greater source of tectonic activity on terrestrial exoplanets in systems of tightly packed planets.

5. Theoretical Uncertainties and Implications

The biggest difference between the tidal stresses acting on short-period exoplanets and mantle convective stresses on the Earth are the timescales over which the stresses vary. The turnover time of the convective eddies in the Earth are of order a million years [Eq. (42)], and the stress from mantle convection continuously pushes a plate in one direction over this timescale. The timescale tidal stresses on short-period exoplanets vary is less than a few years (Secs. 4.1-4.3), and will push a plate in alternating directions over this timescale. Although the magnitudes of tidal forces on a short-period planet's lithosphere may be sufficient to initiate subduction, the fact that the direction these forces push a plate vary rapidly over the planet's lifetime may hinder subduction. We speculate the rapidly varying direction of the tidal force may lead to interesting stick-slip behavior at fault lines, potentially leading to the subduction of plates. Further work is needed to state conclusively that tidal stress aids or hinders the subduction of lithospheric plates.

We assumed the entire planet was a homogeneous, constant density incompressible elastic solid. Although the silicate crust of USP planets may melt to form a surface lava ocean (which will have no shear modulus), these oceans will have depths $\lesssim 1\%$ the planet's radius ([Léger et al., 2011](#)). Unless an USP planet has a lava ocean depth comparable to the planet's radius, the magnitude of the tidal stress calculated in Sections 2 and 4 are unlikely to change by an order of magnitude. However, we note that only the nightsides of USP planets have the right conditions for plate tectonics, since the dayside surfaces are too hot for mantle convection ([van Summeren et al., 2011](#)).

We assumed a constant shear modulus and viscosity characteristic of the cold, terrestrial planets here in our solar system. Both the shear modulus and viscosity of a planet depend on the pressure and temperature of the rocky planet (e.g. [Dziewonski et al. 1975](#); [Yoder 1995](#); [Turcotte and Schubert 2002](#)). Inclusion

of these effects would probably require relaxing our idealized model for a rocky exoplanet and is outside the scope of this work, but will likely not change the magnitude of the tidal strain by more than an order of magnitude.

When simulating plate tectonics with a pseudo-plastic rheology, one typically needs a yield stress of order 10^8 dynes/cm² for convective stresses to be able to subduct plates. It is a well known problem that this is much lower than the yield strength of the rock which make up the Earth’s crust, obtained from laboratory experiments (Kohlstedt et al., 1995; Korenaga, 2013). It has been argued by many surface water is the most promising way to weaken the Earth’s lithospheric plates, since minerals which compose the Earth’s lithosphere are weaker when wet than dry (e.g. Karato et al. 1986; Mei and Kohlstedt 2000a,b). But water by itself may not be able to sufficiently weaken the Earth’s lithospheric yield stress to values which can be overcome by mantle convection stresses. As an example, the experimental work of Chen et al. (1998) shows wet olivine is weakened only an extra $\sim 20\%$ compared to dry olivine in the same high pressure environments expected in the Earth’s lithosphere. This is far short of the order of magnitude drop in yield stress needed for simulations using pseudo-plastic rheologies to see plate-like behavior (e.g. Trompert and Hansen 1998; van Heck and Tackley 2008; Foley and Becker 2009). This idea is further complicated by the fact that the oceanic lithosphere is expected to be dry. Because water is highly soluble in melts, melting beneath mid-ocean ridges dehydrates the oceanic mantle and lithosphere (Hirth and Kohlstedt, 1996). A more promising way to create both localized weak zones and strong plates is the thermal cracking hypothesis of Korenaga (2007), who argues thermal stresses on a cooling early Earth are sufficient to cause deep cracks, and creating localized weak zones when the effective friction coefficient of oceanic plates is reduced due to pore fluid pressure. The presence of surface water on exoplanets is of course a very topical question for understanding the habitability of exoplanets, and it is not clear if surface water is present or absent on the planets considered in this work.

Damage theory, which models the reduction and growth of grains in a deformed lithosphere, is a plausible way to obtain plate-like behavior with a realistic rheology, without invoking surface water to weaken the Earth’s lithosphere (Bercovici and Ricard, 2003; Foley et al., 2012). Recent experimental (Cross and Skemer, 2017) and theoretical (Bercovici and Skemer, 2017) work argues the deformation of two-phase materials which make up the Earth’s lithosphere reduce grain sizes, which lead to localized weak zones forming plate boundaries. The mixing induced by damage is active in the mid lithosphere and efficient in the deep lithosphere, but is ineffective in the shallowest portions of the Earth’s lithosphere (Bercovici and Skemer, 2017). We speculate that within the framework of damage theory, the fast timescales (\lesssim years) over which the tidal stress discussed in Section 4 varies makes healing (growth of grains) almost impossible for every exoplanet of interest ($h, \Delta h \gtrsim 10^{-5}$), at least in the manner Bercovici and Ricard (2014) speculated occurs on Venus because of the high surface temperature of Venus’s lithosphere (explaining why Venus has plate boundaries but not active plate tectonics). However, the fact that these tidal stresses are very un-localized (Fig. 1) leads us to believe tidal stress by itself will not lead to the

formation of sharp plate boundaries, like we have here on Earth. Moreover, it is not clear how rapidly varying tidal stress reduces grain sizes according to the formalism developed by [Bercovici and Ricard \(2012, 2013\)](#). Since mantle convection stresses vary on timescales \gtrsim Myr, the formalism developed by [Bercovici and Ricard \(2012, 2013\)](#) assumes a purely viscous planet rheology, and neglects any mantle or lithosphere elasticity. As we have argued in this work, the lithospheric response to varying tidal stress will be primarily elastic, not viscous. How self-consistent modeling of damage in the lithosphere changes the results presented in Sections 2-4 is outside the scope of this work, but may make tectonic activity more likely for terrestrial exoplanets undergoing significant tidal stress.

Although the exoplanetary model presented in this paper is highly idealized, one could in principal carry out a more detailed calculation of the tidal stress in a planet’s lithosphere with realistic equations of state, given constraints on a planet’s bulk composition and orbit. Such calculations would illuminate the extent tidal stress effectively “weakens” a planet’s lithosphere (or drives subduction outright), compared to planets without such significant sources of tidal stress. If signatures of active plate tectonics were detected (see Sec. 6 for discussion), a population of tidally stressed planets could help geophysicists and planetary scientists differentiate between theories which claim weakening a planet’s lithosphere with surface water or gravity is the main driver of plate tectonics ([O’Neill and Lenardic, 2007](#); [Valencia et al., 2007](#); [Korenaga, 2010](#)), or a steady internal heat source which drives mantle convection (e.g. [Barnes et al. 2009](#)).

6. Prospects for gathering empirical evidence of plate tectonics.

The first, tentative observational evidence that geological processes may be affecting an exoplanet were produced on 55 Cnc e ([Demory et al., 2016](#)). It is likely that others will follow particularly in systems that are optimal to be followed up, such as the many worlds surrounding TRAPPIST-1 ([Gillon et al., 2017](#); [de Wit et al., 2016](#); [Barstow and Irwin, 2016](#); [Morley et al., 2017](#)), or GJ 1132b ([Berta-Thompson et al., 2015](#); [Dittmann et al., 2016](#)).

Two types of observables may be produced on exoplanets: atmospheric, and topographic. Atmospheric information can be gleaned if a planet transits its host star, by performing spectro-photometry at inferior conjunction (transmission spectroscopy), or at superior conjunction (emission spectroscopy) ([Seager and Deming, 2010](#)). In both instances, the chemical content of the atmosphere can be retrieved, however different molecules sometimes have broad overlapping features that can be confused. Alternatively, for transiting and non-transiting planets, specific molecules can be identified (in transmission or emission) using high-resolution spectroscopy ([Snellen et al., 2010](#); [Rodler and López-Morales, 2014](#)). This method can uniquely identify certain molecules, but it struggles to measure relative abundances. Light gases such as SO₂ are produced in large quantities by volcanic eruptions, particularly at zones of subduction, where ex-

plosive, Plinian eruptions can inject SO_2 high into the stratosphere where its released gases could become detectable (e.g. the Pinatubo in 1991).

We have identified a number of planets, with high h values, that are more likely than others to initiate plate tectonics thanks to significant tidal stresses (Appendix B, Table B.3). We invite observers to collect atmospheric data on those, and identify common molecules indicative of plate tectonics from that subpopulation. Once tracers are identified, work can proceed on a wider range of planets in order to explore the role of mass, radius, gravity, or composition, atmospheric pressure, maybe the presence of large volumes of liquid water, on the onset and persistence of plate tectonics. Careful future studies may shed information as to why plates developed on Earth.

For a subset of planets, topographic information may also be reachable thanks to a technique called *eclipse mapping*. As a planet disappears behind its host star (at superior conjunction), its disc is progressively occulted by the star. High-cadence, high precision photometric time-series at ingress and egress can produce two-dimensional brightness maps of an exoplanet (de Wit et al., 2012; Majeau et al., 2012; Loudon and Kreidberg, 2017). Planet-planet occultations may reveal similar information (Luger et al., 2017). Active volcanoes on the surface of Io represent some of the brightest features at mid-infrared wavelengths in the Solar system (Peters and Turner, 2013; de Kleer et al., 2014). Similar phenomena might become observable on planets such as TRAPPIST-1b with the JWST. Geolocating volcanoes on the surface of exoplanets, and examining their distribution may show the outlines of plates just like most volcanoes on Earth exist near subduction zones.

One potential way to infer the presence of “tidally driven” plate tectonics is related to the latitudinal dependence of tidal forces acting on the planet’s plates. Near the equator of the planet, the tidal force is stronger than at the north and south poles (see Fig. 3). Numerical simulations of plate tectonics show the type of tectonic activity depends strongly on the stress and force exerted on a planet’s lithosphere (e.g. Trompert and Hansen 1998; van Heck and Tackley 2008; Foley and Becker 2009). If an exoplanet with latitude-dependent tectonic activity was detected (volcanoes tracing out plates near the equator, volcanically quiet near the poles), this may be a signature of tidally-driven plate tectonics. However, numerical simulations are needed before any concrete predictions are made.

7. Conclusions

What conditions are necessary for the onset and sustenance of plate tectonics is a question of interest to both geophysicists and astrophysicists looking for worlds outside our solar system. Many planets thought to be primarily rocky orbit close ($\lesssim 0.1$ au) to their host stars. By modeling an exoplanet as a constant density, homogeneous, incompressible sphere, we calculate the tidal stresses and strains acting everywhere in the planet (Sec. 2; Fig. 1). We then show when tidal stress is sufficiently strong, tidal forces exerted on lithospheric plates can be stronger than the frictional force between two sliding plates (Sec. 3;

Fig. 3). Tidal forces have the potential to aid mantle convective stresses in subducting lithospheric plates, or drive subduction without the need for mantle convective stresses, initiating plate tectonics on exoplanets. Rocky planet rotating non-synchronously around M-dwarfs, and eccentric Ultra-Short Period ($P_{\text{orb}} \lesssim 1$ day) planets may have interesting tectonic activity due to the significant tidal stress induced on the planet by the host star (Secs. 4.1-4.2). Planet-planet tides in systems of tightly packed inner-planets do not induce sufficient tidal stress to significantly aid tectonic activity. However, we note that these stresses remain significantly larger than the tidal stress on the Earth from the Moon, potentially implying planet-planet tidal interactions at conjunction are capable of triggering Earthquakes on exoplanets (Sec. 4.3). Many uncertainties remain on the plausibility of tidal stress to drive tectonic activity, the biggest being the rapid variation in direction and magnitude of tidal forces exerted on lithospheric plates (Sec. 5). We discuss prospects for gathering observational evidence for tectonic activity on exoplanets in Section 6. This work has implications for the geology and habitability of terrestrial exoplanets orbiting close ($\lesssim 0.1$ au) to their host stars.

Acknowledgements

We thank the anonymous referees whose comments improved the quality and clarity of this work. J. J. Zanazzi thanks Hilke Schlichting, Dong Lai, and Lauren Weiss for useful conversations. Amaury Triaud would like to thank the entire TRAPPIST/SPECULOOS team for avid discussions. JZ is supported in part by a NASA Earth and Space Sciences Fellowship in Astrophysics. We thank United Airlines for their hospitality in providing a venue where a significant portion of this work was initiated, and for their seat allocation algorithm, that placed us next to each other.

References

- Anglada-Escudé, G., and 30 colleagues 2016. A terrestrial planet candidate in a temperate orbit around Proxima Centauri. *Nature* 536, 437-440.
- Auclair-Desrotour, P., Laskar, J., Mathis, S. 2017. Atmospheric tides in Earth-like planets. *Astronomy and Astrophysics* 603, A107.
- Balbus, S. A. 2014. Dynamical, biological and anthropic consequences of equal lunar and solar angular radii. *Proceedings of the Royal Society of London Series A* 470, 20140263-20140263.
- Barnes, R., Jackson, B., Greenberg, R., Raymond, S. N. 2009. Tidal Limits to Planetary Habitability. *The Astrophysical Journal* 700, L30-L33.
- Bartstow, J.K., Irwin, P.G.J. 2016. Habitable worlds with JWST: transit spectroscopy of the TRAPPIST-1 system? *MNRAS* 461, L92.

- Batalha, N. M., and 51 colleagues 2011. Kepler’s First Rocky Planet: Kepler-10b. *The Astrophysical Journal* 729, 27.
- Becker, J. C., Vanderburg, A., Adams, F. C., Rappaport, S. A., Schwengeler, H. M. 2015. WASP-47: A Hot Jupiter System with Two Additional Planets Discovered by K2. *The Astrophysical Journal* 812, L18.
- Berta-Thompson, Z.K. et al. 2015. A rocky planet transiting a nearby low-mass star. *Nature* 527, 204-207.
- Bercovici, D., Ricard, Y. 2014. Plate tectonics, damage and inheritance. *Nature* 508, 513.
- Bercovici, D., Ricard, Y. 2013. Generation of plate tectonics with two-phase grain-damage and pinning: Source-sink model and toroidal flow. *Earth and Planetary Science Letters* 365, 275.
- Bercovici, D., Ricard, Y. 2012. Mechanisms for the generation of plate tectonics by two-phase grain-damage and pinning. *Physics of the Earth and Planetary Interiors* 202, 27.
- Bercovici, D., Ricard, Y. 2003. Energetics of a two-phase model of lithospheric damage, shear localization and plate-boundary formation. *Geophysical Journal International* 152, 581-596.
- Bercovici, D., Skemer, P. 2017. Grain damage, phase mixing and plate-boundary formation. *Journal of Geodynamics* 108, 40.
- Bolmont, E., Selsis, F., Raymond, S. N., Leconte, J., Hersant, F., Maurin, A.-S., Pericaud, J. 2013. Tidal dissipation and eccentricity pumping: Implications for the depth of the secondary eclipse of 55 Cancri e. *Astronomy and Astrophysics* 556, A17.
- Bonfils, X., and 14 colleagues 2017. A temperate exo-Earth around a quiet M dwarf at 3.4 parsecs. *ArXiv e-prints* arXiv:1711.06177.
- Bonfils, X. et al. 2013. The HARPS search for southern extra-solar planets. XXXI. The M-dwarf sample. *Astronomy & Astrophysics* 549, 109.
- Bruntt, H., Deleuil, M., Fridlund, M., Alonso, R., Bouchy, F., Hatzes, A., Mayor, M., Moutou, C., Queloz, D. 2010. Improved stellar parameters of CoRoT-7. A star hosting two super Earths. *Astronomy and Astrophysics* 519, A51.
- Byerlee, J. 1978. Friction of rocks. *Pure and Applied Geophysics* 116, 615.
- Campante, T. L., and 40 colleagues 2015. An Ancient Extrasolar System with Five Sub-Earth-size Planets. *The Astrophysical Journal* 799, 170.
- Carter, J. A., and 45 colleagues 2012. Kepler-36: A Pair of Planets with Neighboring Orbits and Dissimilar Densities. *Science* 337, 556.

- Castan, T., Menou, K. 2011. Atmospheres of Hot Super-Earths. *The Astrophysical Journal* 743, L36.
- Chen J., Inoue T., Weidner D. J., Wu Y., Vaughan M. T., 1998, *GeoRL*, 25, 575
- Correia, A. C. M., Laskar, J., de Surgy, O. N. 2003. Long-term evolution of the spin of Venus. I. theory. *Icarus* 163, 1-23.
- Cross, A. J., Skemer, P. 2017. Ultramylonite generation via phase mixing in high-strain experiments. *Journal of Geophysical Research (Solid Earth)* 122, 1744.
- Dai, F., and 10 colleagues 2015. Doppler Monitoring of the WASP-47 Multi-planet System. *The Astrophysical Journal* 813, L9.
- Dawson, R. I., Fabrycky, D. C. 2010. Radial Velocity Planets De-aliased: A New, Short Period for Super-Earth 55 Cnc e. *The Astrophysical Journal* 722, 937-953.
- Deck, K. M., Holman, M. J., Agol, E., Carter, J. A., Lissauer, J. J., Ragozzine, D., Winn, J. N. 2012. Rapid Dynamical Chaos in an Exoplanetary System. *The Astrophysical Journal* 755, L21.
- Delisle, J.-B., Correia, A. C. M., Leleu, A., Robutel, P. 2017. Spin dynamics of close-in planets exhibiting large TTVs. *ArXiv e-prints* arXiv:1705.04460.
- de Kleer, K. et al. 2014. Near-infrared monitoring of Io and detection of a violent outburst on 29 August 2013. *Icarus* 242, 352-364
- de Wit, J. et al. 2012. Towards consistent mapping of distant worlds: secondary-eclipse scanning of the exoplanet HD 189733b. *Astronomy & Astrophysics* 548, 128.
- de Wit, J. et al. 2016. A combined transmission spectrum of the Earth-sized exoplanets TRAPPIST-1 b and c. *Nature* 537, 69.
- Demory, B.-O., and 13 colleagues 2016. A map of the large day-night temperature gradient of a super-Earth exoplanet. *Nature* 532, 207-209.
- Demory, B.-O., Gillon, M., Madhusudhan, N., Queloz, D. 2016. Variability in the super-Earth 55 Cnc e. *Monthly Notices of the Royal Astronomical Society* 455, 2018-2027.
- Dittmann J.A. et al. 2017. A Search for Additional Bodies in the GJ 1132 Planetary System from 21 Ground-based Transits and a 100-hr Spitzer Campaign. *The Astronomical Journal* 154, 142.
- Dressing, C. D., Charbonneau, D. 2013. The Occurrence Rate of Small Planets around Small Stars. *The Astrophysical Journal* 767, 95.

- Dressing, C. D., Charbonneau, D. 2015. The Occurrence of Potentially Habitable Planets Orbiting M Dwarfs Estimated from the Full Kepler Dataset and an Empirical Measurement of the Detection Sensitivity. *The Astrophysical Journal* 807, 45.
- Dziewonski, A. M., Hales, A. L., Lapwood, E. R. 1975. Parametrically simple Earth models consistent with geophysical data. *Physics of the Earth and Planetary Interiors* 10, 12-48.
- Esteves, L. J., De Mooij, E. J. W., Jayawardhana, R. 2015. Changing Phases of Alien Worlds: Probing Atmospheres of Kepler Planets with High-precision Photometry. *The Astrophysical Journal* 804, 150.
- Fischer, D. A., and 11 colleagues 2008. Five Planets Orbiting 55 Cancri. *The Astrophysical Journal* 675, 790-801.
- Foley, B. J., Becker, T. W. 2009. Generation of plate-like behavior and mantle heterogeneity from a spherical, viscoplastic convection model. *Geochemistry, Geophysics, Geosystems* 10, Q08001.
- Foley, B. J., Bercovici, D., Landuyt, W. 2012. The conditions for plate tectonics on super-Earths: Inferences from convection models with damage. *Earth and Planetary Science Letters* 331, 281-290.
- Fowler, A. C. 1993. Boundary layer theory and subduction. *Journal of Geophysical Research* 98, 21997-22005.
- Fulton, B. J., and 12 colleagues 2017. The California-Kepler Survey. III. A Gap in the Radius Distribution of Small Planets. *The Astronomical Journal* 154, 109.
- Gillon, M., and 14 colleagues 2016. Temperate Earth-sized planets transiting a nearby ultracool dwarf star. *Nature* 533, 221-224.
- Gillon, M., and 29 colleagues 2017. Seven temperate terrestrial planets around the nearby ultracool dwarf star TRAPPIST-1. *Nature* 542, 456-460.
- Ginzburg, S., Schlichting, H. E., Sari, R. 2017. Core-powered mass loss sculpts the radius distribution of small exoplanets. *ArXiv e-prints* arXiv:1708.01621.
- Goldreich, P., Peale, S. 1966. Spin-orbit coupling in the solar system. *The Astronomical Journal* 71, 425.
- Gregg, T. 2015. Planetary Tectonics and Volcanism: The Inner Solar System. *Treatise on Geophysics* (Second Edition) 10, 307-325.
- Guenther, E. W., and 44 colleagues 2017. K2-106, a system containing a metal rich planet and a planet of lower density. *ArXiv e-prints* arXiv:1705.04163.
- Hadden, S., Lithwick, Y. 2016. Kepler Planet Masses and Eccentricities from TTV Analysis. *ArXiv e-prints* arXiv:1611.03516.

- Haywood, R. D., and 14 colleagues 2014. Planets and stellar activity: hide and seek in the CoRoT-7 system. *Monthly Notices of the Royal Astronomical Society* 443, 2517-2531.
- He, M. Y. , Triaud, A. H. M. J. , Gillon, M. 2017. First limits on the occurrence rate of short-period planets orbiting brown dwarfs *Monthly Notices of the Royal Astronomical Society* 464, 2687.
- Hirth, G., Kohlstedt, D. L. 1996. Water in the oceanic upper mantle: implications for rheology, melt extraction and the evolution of the lithosphere. *Earth and Planetary Science Letters* 144, 93.
- Howard, A.W. et al. 2012. Planet Occurrence within 0.25 AU of Solar-type Stars from Kepler. *The Astrophysical Journal Supplements* 201, 15
- Ide, S., Yabe, S. and Tanaka, Y. 2016. Earthquake potential revealed by tidal influence on Earthquake size-frequency statistics. *Nature Geoscience* 9, 834-837.
- Karato, S.-I., Paterson, M. S., Fitzgerald, J. D. 1986. Rheology of synthetic olivine aggregates: Influence of grain size and water. *Journal of Geophysical Research* 91, 8151
- Kasting, J. F., Whitmire, D. P., Reynolds, R. T. 1993. Habitable Zones around Main Sequence Stars. *Icarus* 101, 108-128.
- Kite, E. S., Manga, M., Gaidos, E. 2009. Geodynamics and Rate of Volcanism on Massive Earth-like Planets. *The Astrophysical Journal* 700, 1732-1749.
- Kohlstedt, D. L., Evans, B., Mackwell, S. J. 1995. Strength of the lithosphere: Constraints imposed by laboratory experiments. *Journal of Geophysical Research* 100, 17587-17602.
- Kopparapu, R. K., Ramirez, R. M., SchottelKotte, J., Kasting, J. F., Domagal-Goldman, S., Eymet, V. 2014. Habitable Zones around Main-sequence Stars: Dependence on Planetary Mass. *The Astrophysical Journal* 787, L29.
- Korenaga, J. 2007. Thermal cracking and the deep hydration of oceanic lithosphere: A key to the generation of plate tectonics?. *Journal of Geophysical Research (Solid Earth)* 112, B05408
- Korenaga, J. 2010. On the Likelihood of Plate Tectonics on Super-Earths: Does Size Matter?. *The Astrophysical Journal* 725, L43-L46.
- Korenaga, J. 2013. Initiation and Evolution of Plate Tectonics on Earth: Theories and Observations. *Annual Review of Earth and Planetary Sciences* 41, 117-151.
- Landau, L. D., Lifshitz, E. M. 1959b. Theory of elasticity.

- Leconte, J., Wu, H., Menou, K., Murray, N. 2015. Asynchronous rotation of Earth-mass planets in the habitable zone of lower-mass stars. *Science* 347, 632-635.
- Lee, E. J., Chiang, E. 2017. Magnetospheric Truncation, Tidal Inspiral, and the Creation of Short and Ultra-Short Period Planets. ArXiv e-prints arXiv:1702.08461.
- Léger, A., and 160 colleagues 2009. Transiting exoplanets from the CoRoT space mission. VIII. CoRoT-7b: the first super-Earth with measured radius. *Astronomy and Astrophysics* 506, 287-302.
- Léger, A., and 25 colleagues 2011. The extreme physical properties of the CoRoT-7b super-Earth. *Icarus* 213, 1-11.
- Lingam, M., Loeb, A. 2017. Implications of tides for life on exoplanets. ArXiv e-prints arXiv:1707.04594.
- Lissauer, J. J., and 38 colleagues 2011. A closely packed system of low-mass, low-density planets transiting Kepler-11. *Nature* 470, 53-58.
- Lissauer, J. J., and 23 colleagues 2012. Almost All of Kepler's Multiple-planet Candidates Are Planets. *The Astrophysical Journal* 750, 112.
- Louden, T., Kreidberg, L. 2017. SPIDERMAN: an open-source code to model phase curves and secondary eclipses. ArXiv e-prints arXiv:171100494
- Luger, R., Lustig-Yaeger, J., Agol, E. 2017. Planet-Planet Occultations in TRAPPIST-1 and Other Exoplanet Systems. ArXiv e-prints arXiv:1711.05739.
- MacDonald, M. G., and 12 colleagues 2016. A Dynamical Analysis of the Kepler-80 System of Five Transiting Planets. *The Astronomical Journal* 152, 105.
- Majeau, C. , Agol, E. , Cowan, N. B. 2012. A Two-dimensional Infrared Map of the Extrasolar Planet HD 189733b. *The Astrophysical Journal Letters* 747, 20.
- Makarov, V. V., Berghea, C., Efroimsky, M. 2012. Dynamical Evolution and Spin-Orbit Resonances of Potentially Habitable Exoplanets: The Case of GJ 581d. *The Astrophysical Journal* 761, 83.
- Mayor, M. et al. 2011. The HARPS search for southern extra-solar planets XXXIV. Occurrence, mass distribution and orbital properties of super-Earths and Neptune-mass planets. ArXiv e-prints arXiv:1109.2497
- Mei, S., Kohlstedt, D. L. 2000. Influence of water on plastic deformation of olivine aggregates: 1. Diffusion creep regime. *Journal of Geophysical Research* 105, 21,457.

- Mei, S., Kohlstedt, D. L. 2000. Influence of water on plastic deformation of olivine aggregates: 2. Dislocation creep regime. *Journal of Geophysical Research* 105, 21,471.
- Moresi, L., Solomatov, V. 1998. Mantle convection with a brittle lithosphere: thoughts on the global tectonic styles of the Earth and Venus. *Geophysical Journal International* 133, 669.
- Morley, C. V. et al. 2017. Observing the Atmospheres of Known Temperate Earth-sized Planets with JWST. *ArXiv e-prints* arXiv:1708.04239
- Morton, T. D., Swift, J. 2014. The Radius Distribution of Planets around Cool Stars. *The Astrophysical Journal* 791, 10.
- Nelson, B. E., Ford, E. B., Wright, J. T., Fischer, D. A., von Braun, K., Howard, A. W., Payne, M. J., Dindar, S. 2014. The 55 Cancri planetary system: fully self-consistent N-body constraints and a dynamical analysis. *Monthly Notices of the Royal Astronomical Society* 441, 442-451.
- Noack, L., Breuer, D. 2014. Plate tectonics on rocky exoplanets: Influence of initial conditions and mantle rheology. *Planetary and Space Science* 98, 41-49.
- Nutzman, P., Charbonneau, D. 2008. Design Considerations for a Ground-Based Transit Search for Habitable Planets Orbiting M Dwarfs. *Publications of the Astronomical Society of the Pacific* 120, 317.
- O'Neill, C., Lenardic, A. 2007. Geological consequences of super-sized Earths. *Geophysical Research Letters* 34, L19204.
- O'Rourke, J. G., Korenaga, J. 2012. Terrestrial planet evolution in the stagnant-lid regime: Size effects and the formation of self-destabilizing crust. *Icarus* 221, 1043-1060.
- Owen, J. E., Wu, Y. 2017. The evaporation valley in the Kepler planets. *ArXiv e-prints* arXiv:1705.10810.
- Papaloizou, J. C. B., Szuszkiewicz, E., Terquem, C. 2017. The TRAPPIST-1 system: Orbital evolution, tidal dissipation, formation and habitability. *ArXiv e-prints* arXiv:1711.07932.
- Peters, M. A., Turner, E. L. 2013. On the Direct Imaging of Tidally Heated ExoMoons. *The Astrophysical Journal* 769, 98.
- Quillen, A. C., Giannella, D., Shaw, J. G., Ebinger, C. 2016. Crustal failure on icy Moons from a strong tidal encounter. *Icarus* 275, 267-280.
- Rodler, F., López-Morales, M. 2014. Feasibility Studies for the Detection of O₂ in an Earth-like Exoplanet. *The Astrophysical Journal* 781, 54

- Ribas, I., and 11 colleagues 2016. The habitability of Proxima Centauri b. I. Irradiation, rotation and volatile inventory from formation to the present. *Astronomy and Astrophysics* 596, A111.
- Rodríguez, A., Callegari, N., Correia, A. C. M. 2016. Coupled orbital and spin evolution of the CoRoT-7 two-planet system using a Maxwell viscoelastic rheology. *Monthly Notices of the Royal Astronomical Society* 463, 3249-3259.
- Rogers, L. A. 2015. Most 1.6 Earth-radius Planets are Not Rocky. *The Astrophysical Journal* 801, 41.
- Schneider, J., Dedieu, C., Le Sidaner, P., Savalle, R., Zolotukhin, I. 2011. Defining and cataloging exoplanets: the exoplanet.eu database. *Astronomy and Astrophysics* 532, A79.
- Seager, S., Deming, D. 2010. Exoplanet Atmospheres. *Annual Review of Astronomy & Astrophysics* 48, 631-672.
- Seager, S., Kuchner, M., Hier-Majumder, C. A., Militzer, B. 2007. Mass-Radius Relationships for Solid Exoplanets. *The Astrophysical Journal* 669, 1279-1297.
- Sinukoff, E., and 22 colleagues 2017. K2-66b and K2-106b: Two extremely hot sub-Neptune-size planets with high densities. *ArXiv e-prints* arXiv:1705.03491.
- Shields, A. L., Ballard, S., Johnson, J. A. 2016. The Habitability of Planets Orbiting M-dwarf Stars. *ArXiv e-prints* arXiv:1610.05765.
- Sinukoff, E., and 21 colleagues 2017. Mass Constraints of the WASP-47 Planetary System from Radial Velocities. *The Astronomical Journal* 153, 70.
- Sleep, N. H. 2012. Maintenance of permeable habitable subsurface environments by Earthquakes and tidal stresses. *International Journal of Astrobiology* 11, 257-268.
- Southam, G., Westall, F. and Spohn, T. 2015. Geology, Life, and Habitability. *Treatise on Geophysics (Second Edition)* 10, 473-486.
- Snellen, I.A.G. et al. 2010. *Nature* 465, 1049-1051.
- Stamenković, V., Noack, L., Breuer, D., Spohn, T. 2012. The Influence of Pressure-dependent Viscosity on the Thermal Evolution of Super-Earths. *The Astrophysical Journal* 748, 41.
- Swift, J. J., Johnson, J. A., Morton, T. D., Crepp, J. R., Montet, B. T., Fabrycky, D. C., Muirhead, P. S. 2013. Characterizing the Cool KOIs. IV. Kepler-32 as a Prototype for the Formation of Compact Planetary Systems throughout the Galaxy. *The Astrophysical Journal* 764, 105.

- Tosi, N., Godolt, M., Stracke, B., Ruedas, T., Grenfell, J. L., Höning, D., Nikolaou, A., Plesa, A.-C., Breuer, D., Spohn, T. 2017. The habitability of a stagnant-lid Earth. ArXiv e-prints arXiv:1707.06051.
- Trompert, R., Hansen, U. 1998. Mantle convection simulations with rheologies that generate plate-like behaviour. *Nature* 395, 686-689.
- Turcotte D. L., Oxburgh E. R., 1967, *JFM*, 28, 29
- Turcotte, D. L., Schubert, G. 2002. *Geodynamics - 2nd Edition*. *Geodynamics - 2nd Edition*, by Donald L. Turcotte and Gerald Schubert, pp. 472. Cambridge University Press, April 2002. ISBN-10: 0521661862. ISBN-13: 9780521661867. LCCN: QE501 .T83 2002 472.
- Turtle, E. P., Jaeger, W. L., Schenk, P. M. 2007. Ionian mountains and tectonics: Insights into what lies beneath Io's lofty peaks. *Io After Galileo: A New View of Jupiter's Volcanic Moon* 109.
- Valencia, D., O'Connell, R. J. 2009. Convection scaling and subduction on Earth and super-Earths. *Earth and Planetary Science Letters* 286, 492-502.
- Valencia, D., O'Connell, R. J., Sasselov, D. D. 2007. Inevitability of Plate Tectonics on Super-Earths. *The Astrophysical Journal* 670, L45-L48.
- van Heck, H. J., Tackley, P. J. 2008. Planforms of self-consistently generated plates in 3D spherical geometry. *Geophysical Research Letters* 35, L19312.
- van Summeren, J., Conrad, C. P., Gaidos, E. 2011. Mantle Convection, Plate Tectonics, and Volcanism on Hot Exo-Earths. *The Astrophysical Journal* 736, L15.
- Vinson, A. M., Hansen, B. M. S. 2017. On the Spin States of Habitable Zone Exoplanets Around M Dwarfs: The Effect of a Near-Resonant Companion. ArXiv e-prints arXiv:1705.09685.
- Weiss, L. M., and 10 colleagues 2016. Revised Masses and Densities of the Planets around Kepler-10. *The Astrophysical Journal* 819, 83.
- Weiss, L. M., and 11 colleagues 2016. Mass and Eccentricity Constraints in the WASP-47 Planetary System from a Simultaneous Analysis of Radial Velocities Transit Timing Variations. ArXiv e-prints arXiv:1612.04856.
- Weller, M. B., Lenardic, A. 2012. Hysteresis in mantle convection: Plate tectonics systems. *Geophysical Research Letters* 39, L10202.
- Wong, T., Solomatov, V. S. 2015. Towards scaling laws for subduction initiation on terrestrial planets: constraints from two-dimensional steady-state convection simulations. *Progress in Earth and Planetary Science* 2, 18.
- Wu, Y., Goldreich, P. 2002. Tidal Evolution of the Planetary System around HD 83443. *The Astrophysical Journal* 564, 1024-1027.

Wu, Y., Lithwick, Y. 2013. Density and Eccentricity of Kepler Planets. *The Astrophysical Journal* 772, 74.

Yoder, C. F. 1995. Venus' free obliquity.. *Icarus* 117, 250-286.

Zanazzi, J. J., Lai, D. 2017. Triaxial deformation and asynchronous rotation of rocky planets in the habitable zone of low-mass stars. *Monthly Notices of the Royal Astronomical Society* 469, 2879-2885.

Appendix A. Explicit Calculation of Strain Amplitude

Decomposing the symmetric tensor \mathbf{u} into spherical coordinates ([Landau and Lifshitz, 1959b](#)), we may write Eq. (27) as

$$u^2 = \frac{1}{2} (u_{rr}^2 + u_{\theta\theta}^2 + u_{\varphi\varphi}^2) + u_{\theta\varphi}^2 + u_{r\theta}^2 + u_{\varphi r}^2. \quad (\text{A.1})$$

Letting $i, j \in \{r, \theta, \varphi\}$, we may decompose u_{ij} as

$$u_{ij} = u_{ij;20} + 2u_{ij;22}, \quad (\text{A.2})$$

where $u_{ij;lm}$ denotes a strain term proportional to the displacements $\xi_{r;lm}$ and $\xi_{\perp;lm}$ [see Eq. (14)]. Explicitly, we have

$$u_{rr;20} = A_{20} \frac{d\xi_{r;20}}{dr} (3 \cos^2 \theta - 1), \quad (\text{A.3})$$

$$u_{\theta\theta;20} = A_{20} \frac{\xi_{r;20}}{r} (3 \cos^2 \theta - 1) - 6A_{20} \frac{\xi_{\perp;20}}{r} (\cos^2 \theta - \sin^2 \theta), \quad (\text{A.4})$$

$$u_{\varphi\varphi;20} = -6A_{20} \frac{\xi_{\perp;20}}{r} \cos^2 \theta + A_{20} \frac{\xi_{r;20}}{r} (3 \cos^2 \theta - 1), \quad (\text{A.5})$$

$$u_{\theta\varphi;20} = u_{\varphi r;20} = 0, \quad (\text{A.6})$$

$$u_{r\theta;20} = -3A_{20} \left(\frac{d\xi_{\perp;20}}{dr} - \frac{\xi_{\perp;20}}{r} + \frac{\xi_{r;20}}{r} \right) \cos \theta \sin \theta, \quad (\text{A.7})$$

and

$$u_{rr;22} = A_{22} \frac{d\xi_{r;22}}{dr} \sin^2 \theta \cos 2\varphi, \quad (\text{A.8})$$

$$u_{\theta\theta;22} = A_{22} \frac{\xi_{r;22}}{r} \sin^2 \theta \cos 2\varphi + 2A_{22} \frac{\xi_{\perp;22}}{r} (\cos^2 \theta - \sin^2 \theta) \cos 2\varphi, \quad (\text{A.9})$$

$$u_{\varphi\varphi;22} = A_{22} \frac{\xi_{r;22}}{r} \sin^2 \theta \cos 2\varphi - 2A_{22} \frac{\xi_{\perp;22}}{r} (\cos^2 \theta - \sin^2 \theta) \cos 2\varphi, \quad (\text{A.10})$$

$$u_{\theta\varphi;22} = -2A_{22} \frac{\xi_{\perp;22}}{r} \cos \theta \sin 2\varphi, \quad (\text{A.11})$$

$$u_{r\theta;22} = A_{22} \left(\frac{d\xi_{\perp;22}}{dr} - \frac{\xi_{\perp;22}}{r} + \frac{\xi_{r;22}}{r} \right) \sin \theta \cos \theta \cos 2\varphi, \quad (\text{A.12})$$

$$u_{\varphi r;22} = -A_{22} \left(\frac{\xi_{r;22}}{r} + \frac{d\xi_{\perp;22}}{dr} - \frac{\xi_{\perp;22}}{r} \right) \sin \theta \sin 2\varphi, \quad (\text{A.13})$$

where

$$A_{20} = \sqrt{\frac{5}{16\pi}}, \quad A_{22} = \sqrt{\frac{15}{32\pi}}. \quad (\text{A.14})$$

Appendix B. Calculation of tidal stresses for known exoplanets

Name	m (M_{\oplus})	R (R_{\oplus})	P_{orb} (days)	M (M_{\odot})	h ($\times 10^{-5}$)
CoRoT-7 b	4.74	1.49	0.85	0.93	228.24
EPIC 246393474 b	5.31	1.50	0.28	0.66	2044.65
GJ 1132 b	1.62	1.13	1.63	0.181	50.93
GJ 9827 b	8.20	1.60	1.21	0.66	98.31
GJ 9827 c	2.51	1.26	3.65	0.66	11.36
HD 3167 b	5.02	1.67	0.96	0.08	212.19
K2-106 b	8.36	1.49	0.57	0.93	365.85
KOI-1843 b	0.32	0.57	0.18	0.46	2045.96
KOI-2700 b	0.86	1.04	0.91	0.63	128.56
Kepler-10 b	3.33	1.44	0.84	0.91	245.87
Kepler-100 b	7.34	1.28	6.89	1.11	1.87
Kepler-102 b	0.41	0.46	5.29	0.81	1.89
Kepler-102 d	2.61	1.14	10.31	0.81	1.22
Kepler-105 c	4.45	1.28	7.13	1.28	2.52
Kepler-114 b	7.00	1.16	5.19	0.71	2.62
Kepler-20 e	3.08	0.85	6.10	0.91	1.64
Kepler-21 b	5.09	1.60	2.79	1.34	23.63
Kepler-338 e	8.58	1.55	9.34	1.10	1.48
Kepler-406 b	6.36	1.40	2.43	1.07	21.28
Kepler-406 c	2.71	0.83	4.62	1.07	3.03
Kepler-408 b	6.36	0.80	2.57	1.08	4.14
Kepler-42 b	2.86	0.77	1.21	0.13	34.02
Kepler-42 c	1.91	0.71	0.45	0.13	278.01
Kepler-42 d	0.95	0.56	1.86	0.13	15.03
Kepler-445 b	6.36	1.55	2.98	0.18	17.45
Kepler-445 d	3.50	1.23	8.15	0.18	1.99
Kepler-446 b	4.45	1.47	1.57	0.22	67.67
Kepler-446 c	2.86	1.08	3.04	0.22	12.16
Kepler-446 d	3.18	1.32	5.15	0.22	5.80
Kepler-60 b	4.19	1.68	7.13	1.10	3.97
Kepler-62 b	8.90	1.28	5.71	0.69	2.34
Kepler-70 b	4.45	0.75	0.24	0.50	539.53
Kepler-70 c	0.67	0.86	0.34	0.50	794.95
Kepler-78 b	1.69	1.17	0.36	0.81	1109.18
Kepler-93 b	4.00	1.45	4.73	0.91	7.51
LP 358-499 b	2.19	1.28	3.07	0.52	16.35
LP 358-499 c	3.18	1.45	4.87	0.52	7.35
TRAPPIST-1 b	0.86	1.06	1.51	0.08	46.49
TRAPPIST-1 c	1.38	1.03	2.42	0.08	21.11
TRAPPIST-1 d	0.41	0.76	4.05	0.08	4.47
TRAPPIST-1 e	0.64	0.90	6.10	0.08	2.46
TRAPPIST-1 f	0.67	1.02	9.21	0.08	1.08

Table B.3: Exoplanets with $m < 10 M_{\oplus}$, $R < 1.6 R_{\oplus}$, and $h > 10^{-5}$ [Eq. (45)], gathered from the [Extrasolar Planets Encyclopaedia](#) database (Schneider et al., 2011). Here, m is the planet’s mass, R is the planet’s radius, P_{orb} is the planet’s orbital period, and M is the host star’s mass. The planet’s semi-major axis is computed via $a = (2\pi/P_{\text{orb}})^{2/3}(GM)^{1/3}$, and we take $\mu = 10^{12}$ dynes/cm² for all bodies.